Fuel Processing Technology 92 (2011) 1675–1684

Contents lists available at ScienceDirect

Fuel Processing Technology

journal homepage: www.elsevier.com/locate/fuproc

Optimal process conditions for the isomerization–cracking of long-chain *n*-paraffins to high octane isomerizate gasoline over Pt/SO_4^{2-}–ZrO_2 catalysts

M. Busto, C.R. Vera, J.M. Grau *

Instituto de Investigaciones en Catálisis y Petroquímica – INCAPE – (FIQ-UNL, CONICET), Santiago del Estero 2654, 3000 Santa Fe, Argentina

ARTICLE INFO

Article history:
Received 5 July 2010
Received in revised form 19 December 2010
Accepted 8 April 2011
Available online 24 May 2011

Keywords:
Sulfate-zirconia
Reaction conditions
n-hexadecane
Cracking
Isomerization
Gasoline

ABSTRACT

An assessment of the process conditions for the isomerization–cracking of long-chain *n*-paraffins over commercial Pt/SO_4^{2-}–ZrO_2 catalysts was made. Pretreatment and reaction conditions were optimized with a focus on the maximization of the yield of short, high octane branched paraffins for the gasoline pool. While selectivity was an important issue attention was also paid to the reduction of the yield to gases (C_1-C_4). Therefore cracking had to be modulated to produce the correct molecular size adjustment without scission to too much smaller fragments. Skeletal isomerization was to be maximized. The activity in both acid-catalyzed reactions had to be tuned while keeping a stable activity level.

The only pretreatment condition assessed was the calcination temperature (screened in the 600–800 °C range). Calcination at 600 °C produced the highest activity level while 700 °C was convenient from the point of view of selectivity. The optimum temperature coincided with the production of the highest concentration of Brönsted acid sites.

Regarding the reaction conditions, increasing temperature values augmented the conversion but also increased the cracking. Therefore optimum values were found at a moderate temperature, 225 °C, given the high reactivity of the feed. Space velocity values were analyzed with attention to the liquid C_{5+} yield, the selectivity to branched isomers and the stability of the catalysts. Best yields to branched naphtha products were obtained at WHSV = 18 h^{-1}. The H_2/hydrocarbon molar ratio was a function of the catalyst coking rate. A value of 10 was enough to attain a stable conversion value. The values of liquid yield as a function of pressure displayed a volcano pattern that was rationalized in terms of a non-classical bifunctional mechanism of reaction. High pressure values increased the concentration of Brönsted acid sites and hence the activity while high pressures enhanced hydrocracking and decreased the liquid yield. The optimal pressure value was 20 atm.

1. Introduction

Isomerization–cracking of long-chain normal paraffins has lately attracted the interest of academy and industry researchers because of its potential impact on augmenting the throughput of middle distillates by means of the processing of low-grade waxy feed stocks coming from the dewaxing of lubes, the recycling of some plastics and the separation of Fischer–Tropsch waxes and heavy paraffins. Most scientific studies have concentrated on the production of naphtha cuts while applications for producing the full range of middle distillates can be found in the patents literature. The catalysts employed in isomerization–cracking are bifunctional. They comprise a metal function supplied by tiny Pt or Pd metal particles and an acid function supplied by the support. Many examples can be found in the literature of catalyst supports for this reaction. They are amorphous aluminosilicates [1–3], zeolites of uni- or multi-directional channels like β, mordenite, L, Y, ZSM-5, ZSM-12, ZSM-22 [4–11], silica alumina phosphates (SAPO) [12,13], mesoporous materials like Al-MCM-41 [14] and oxoanion promoted zirconia, SO_4^{2-}–ZrO_2 WO_3–ZrO_2 and SO_4^{2-}–WO_3–ZrO_2 [15–21]. A review on the available catalysts for hydroisomerization of long-chain normal paraffins has been recently published [22].

Researchers were early confronted with the fact that conventional hydrocracking catalysts like silica-alumina or β and L zeolites, were not appropriate for the treatment of highly paraffinic feed stocks. Too much cracking on these catalysts produced a high yield of low-value light gases with a consequent decrease of the liquid yield and the fuel throughput of the process.

Especially when the desired products are gasoline compounds the requirements on the catalysts become stringent. For producing a gasoline product the molecules of the feed must be more or less severely cracked to the C_5–C_{12} range and skeletically isomerized to produce a maximum of branches. Skeletal branching is closely related to the antidetonating capacity of the gasoline. Both skeletal isomerization and cracking are acid-catalyzed reactions, i.e. they proceed over acid sites.

* Corresponding author at: INCAPE, Santiago del Estero 2654, 3000 Santa Fe, Argentina. Tel.: +54 342 4533858; fax: +54 342 4531068.
E-mail address: jgrau@fiq.unl.edu.ar (J.M. Grau).

0378-3820/$ – see front matter © 2011 Elsevier B.V. All rights reserved.
doi:10.1016/j.fuproc.2011.04.010

The first catalytic issue is therefore the correct distribution of acid strength of these catalysts. Acidity requirements grow inversely proportional to the length of the chain with the general understanding that the longer the chain the higher the reactivity of the paraffin. Cracking is always more demanding that skeletal branching. This is one reason why cracking can sometimes proceed after skeletal branching has taken place on a same acid site. The consequences of an inappropriate acid strength distribution are easily foreseen. If the acid sites are too strong extensive cracking occurs with the combined disadvantages of low liquid yield and premature catalyst coke fouling. If the acid sites are too weak isomerization might occur but cracking will be highly disfavored. As a consequence inconveniently long isomers of low volatility and low octane number are obtained.

In the search for a correct isomerization–cracking catalyst both common isomerization and cracking catalysts have been tried. While cracking catalysts have proved not to provide adequate liquid yield and selectivity, isomerization catalysts have been more suitable (see Table 1).

High liquid yields and high selectivity to branched isoparaffins can notably be obtained over oxoanion promoted zirconia catalysts. These catalysts, tungsten–zirconia (WO_3–ZrO_2) and sulfate–zirconia (SO_4^{2-}–ZrO_2) have outstanding properties of high activity and selectivity at low temperatures. Many reports have been published on the catalytic properties of these two catalysts for the isomerization and cracking of medium and long paraffins. These reports have unfortunately concentrated on the study of a few synthesis or reaction variables. A comprehensive study on the influence of the full range of variables needed for running a hydrocracking process is still lacking.

A comprehensive assessment of reaction variables for the isomerization–cracking of long paraffins over commercial SO_4^{2-}–ZrO_2 is done in this work using n-hexadecane as a model compound. Reaction, pressure, hydrogen-to-hydrocarbon molar ratio and spatial velocity are screened in the convenient ranges in order to optimize the relevant merit figures of the process: octane properties of the isomerizate, liquid yield, appropriate stability of the catalyst, etc. A pretreatment variable related to the activity and selectivity of the catalyst was also screened, the calcination temperature of the support. No other pretreatment was deemed necessary since only available commercial catalysts are used and calcination temperature is the variable that affects the most the final acidity distribution.

In order to correctly focus the development of the work a previous discussion on the relation of molecular features, thermodynamics, octane number and overall gasoline quality issues was inserted in the beginning of the Results and discussion section. Such recalling of concepts seems necessary to correctly perform the optimization procedure.

2. Experimental

2.1. Catalysts preparation

A commercial SO_4^{2-}–ZrO_2 support (MEL Chemicals) in the form of a powdery sulphate doped hydroxide gel (Grade XZO 1249/01, 7 wt.% SO_3 on ZrO_2 basis, 5 microns average particle size, >300 $m^2\ g^{-1}$, >0.3 ml g^{-1}) was used. This powder was first pressed and shaped into cylindrical pellets using a die and a hydraulic press (8 Tn cm^{-2}). Then the pellets were ground and sieved to 35–80 meshes. Samples were taken and were subjected to calcination in static air (3 h) in a muffle at several calcination temperatures (Tc), 600, 700 and 800 °C in order to see the influence of this variable on acidity, crystal structure, catalytic activity and selectivity. In each calcination treatment the catalyst was first heated from room temperature to 180 °C at 2 °C min^{-1} in air and this value was held for 1 h. Then the temperature was increased in 1 h to the desired value of Tc, (600, 700, 800 °C) and held for another 2 h. The sample was then cooled down to room temperature and unloaded. The obtained SO_4^{2-}–ZrO_2 crystalline solid was named SZ^{Tc}.

SZ^{Tc} was then impregnated with chloroplatinic acid by the incipient wetness method. The amount of solution was regulated in order to obtain 0.5% Pt in the final catalyst. This Pt load was chosen in attention to some previous reports on the influence of the Pt content on the performance of the catalyst [23]. Once impregnated the sample was kept 24 h at room temperature. Then it was put in a stove and the temperature was raised slowly from room temperature to 110 °C. Finally it was dried at this temperature overnight. The dried material was then calcined in static air (3 h) in a muffle at 500 °C and cooled down in nitrogen. The metal phase was reduced by placing the sample in a hydrogen stream (80 ml.min^{-1}) and heating at 300 °C for 1 h. The thus obtained samples were called $PtSZ^{Tc}$. The temperature of reduction was chosen in accord with previous studies of TPR of Xu and Sachtler [24] that indicated the ranges of sulfate decomposition. In order to match the temperatures of possible sulfur decomposition and metal sintering, the maximum temperature of reaction (300 °C) was made to coincide with the temperature of the reduction step.

2.2. Catalysts physicochemical characterization

The catalysts were characterized by means of element chemical analysis, X-ray diffraction (crystallinity and crystal phase), nitrogen

Table 1
Results related to the hydrocracking of long paraffins over different catalysts.

Catalyst	T [°C]	Feed	H_2/Feed [mole ratio]	PH_2 [atm]	WHSV [h^{-1}]	X [%]	S_{iso} [%]	S_{C1-C4} [%]	Ref.
0.6Pt/MSA	285	n-C_{10}	4	29.6	1.46	50.0	79.0	–	[3]
0.5Pt/CaY	275	n-C_9		2.2	1.00	76.4	87.8	12.2	[9]
0.5Pt/H-USY	290	n-C_8	16	6.8	0.42–112[a]	55.7	92.6	6.9	[5]
0.5Pt/H-β	290	n-C_8	16	6.8	0.42–112[a]	47.6	77.1	20.1	[5]
0.5Pt/H-LTL	290	n-C_8	16	6.8	0.42–112[a]	49.7	72.4	26.2	[5]
0.3Pt/H-MOR	300	n-C_8	6	14.8	4.00	67.9	24.2	71.6	[10]
0.5Pt/H-MOR	235	n-C_{13-20}	12	19.7	3.00	62.9	37.8	25.0	[13]
H-MOR+Pt/Al_2O_3	300	n-C_8	6	14.8	4.00	79.3	61.6	67.4	[10]
Pt/H-MOR+Al_2O_3	300	n-C_8	6	14.8	4.00	50.4	55.0	52.3	[10]
0.5Pt/H-ZSM-5	280	n-C_9	6	1.9	1.00	98.5	18.9	–	[11]
0.5Pt/H-ZSM-12	290	n-C_8	16	6.8	0.42-112[a]	50.5	66.8	27.5	[5]
0.5Pt/H-ZSM-22	290	n-C_{12}	7	59.2	1.04	93.0	90.0	–	[6]
0.5Pt/SAPO-11	371	n-C_{13-20}	12	9.9	3.00	79.7	58.0	22.2	[13]
0.5Pt/ WO_3-ZrO_2	230	n-C_{16}	2	20.4	1.00	85.9	83.1	–	[15]
0.5Pt/WO_3-ZrO_2	300	n-C_{10}	6	0.99	1.00	98.0	55.3	36.7	[20]
0.5Pt/ SO_4-ZrO_2	150	n-C_{16}	2	20.4	1.00	76.7	19.8	–	[15]
1.0Pt/SO_4-ZrO_2	300	n-C_{10}	6	14.8	4.00	89.3	38.7	39.1	[21]
Pd/Al-MCM-41	350	n-C_{13}	6.5	34.5	1.50	60.2	86.5	–	[14]

PH_2: hydrogen partial pressure; X: conversion; S_{iso}: selectivity to isoparaffins; S_{C1-C4}: selectivity to light gases; [a]: range varied in order to obtain approximately 50% conversion.

adsorption (specific surface area and pore volume distribution), temperature programmed desorption of adsorbed pyridine (TPD-Py) (amount and strength of acid sites) or FTIR-Py (type of acid sites) and n-hexadecane test batch reaction (activity, selectivity). The properties of the metal phase were assessed by the test reaction of cyclohexane dehydrogenation.

The Pt content of the catalysts was determined by atomic emission spectroscopy (ICP-AES) using an ARL 3410 equipment. Before ICP analysis the solids were dissolved in a digestive pump with a mixture of 1 ml sulfuric acid, 3 ml chlorhydric acid and 1 ml nitric acid. The S content was determined in a LECO CS600-Series analyzer using combustion and infrared detection of the evolved gases.

X-ray diffraction spectra were measured in a Shimadzu XD-1 equipment with CuKα radiation filtered with Ni. The spectra were recorded in the 2θ range between 20 and 65° and with a scanning rate of 1.2° min^{-1}. The percentage of tetragonal phase of the samples was calculated using Eq. (1) [25]. The peaks located at 2θ = 28° and 2θ = 31° were attributed to the monoclinic phase of zirconia and those located at 2θ = 30° to the tetragonal phase. The quantification of the monoclinic and tetragonal phases was done by using a equation given below:

$$T(\%) = 100\,\alpha\,It / (Im + \alpha\,It) \quad (1)$$

where: T (%) = content of the tetragonal phase; α = 0.81; It = integrated intensity corresponding to the (111) tetragonal peak and Im = sum of the integrated intensities of the (111) and (11–1) monoclinic peaks.

The quantification of the amount of each crystalline phase and the amount of amorphous matter was made by Rietveld Quantitative Analysis (RQA). From these values the crystallinity percentage and the crystal size (tc) were calculated. Calibration constants were computed from reliable structural data.

The textural properties of the catalysts were determined from nitrogen physisorption data. Nitrogen adsorption was performed in a Micromeritics 2100 E equipment. The specific surface area (Sg) was determined from data of the adsorption branch of nitrogen at 77 K using BET analysis. The pore distribution was determined by the BJH method with data of the desorption branch [26].

The amount and strength of acid sites were assessed by means of TPD of pyridine (Merck, 99.9%). The samples (0.2 g) were first activated in flowing dry air (60 ml min^{-1}) for 1 h at 500 °C and then they were cooled in dry nitrogen to room temperature and immersed in a vial containing pure pyridine. The vial was closed and left for 4 h. Then the vial was opened and the samples were filtered and dried in still air at room temperature. The samples were then placed in a quartz micro reactor and stabilized in N_2 for 1 h at 100 °C. Then they were heated from this temperature to 700 °C at 10 °C min^{-1}. The desorbed products were continuously analyzed in a flame ionization detector and the signal recorded in a computer connected on-line. The acid sites were classified as weak, mild or strong depending on the range of desorption of pyridine. Sites desorbing between 100 and 250 °C were considered "weak" acid sites. Sites desorbing between 250 and 400 °C were considered "mild" and sites desorbing between 400 and 700 °C were considered "strong".

The type of acidity (Brönsted or Lewis) was measured by FT-IR absorption spectroscopy of adsorbed pyridine (Merck, 99.9%). The adsorption was performed in an all-glass equipment with an IR cell. The adsorbed amount was assessed by infrared absorption in the 1400–1600 cm^{-1} range using a Nicolet Avatar 3600 FT-IR spectrometer (resolution 2 cm^{-1}). Catalyst self supported circular wafers (2 cm diameter, 0.05 g) were used for the tests. They were first activated in flowing dry air (60 ml min^{-1}) for 1 h at 500 °C and then vacuum treated at the same temperature for 30 min in a cell with KCl windows to a residual pressure lower than 10^{-5} Torr. In order to verify the generation of Brönsted dynamic acid sites with the reduction pretreatment some samples were activated in air, stripped in nitrogen, reduced in hydrogen at 300 °C for 1 h and finally degassed in vacuo. Pyridine was introduced in the cell at 5 Torr pressure at 100 °C for 15 min then outgassed at 10^{-5} Torr maintaining the temperature for 30 min. The IR spectra were carried out at room temperature after (i) the activation period in dry air, (ii) the reduction period in hydrogen and (iii) after pyridine desorption in vacuum at 10^{-5} Torr during 1 h at 100 °C. Finally the spectrum of pyridine was obtained by subtracting (iii) from (i) or (ii).

2.3. Reaction tests

2.3.1. Cyclohexane dehydrogenation

The catalytic properties of the metal function were also evaluated using these test reaction. The dehydrogenation of cyclohexane (CH) to benzene is a structure insensitive reaction. The activity is known to be strictly proportional to the number of surface active sites. The test was performed using the following conditions: catalyst mass = 0.1 g, 300 °C, 1 atm, molar ratio H_2/CH = 16, WHSV = 12.6 h^{-1}. Cyclohexane was supplied by Merck (spectroscopy grade, 99.9% pure). The specified sulfur upper limit was 0.001%. A tubular quartz reactor with an internal diameter of 10 mm was used.

2.3.2. n-Hexadecane isomerization–cracking

The screening of reaction conditions was performed using the test of isomerization–cracking of n-hexadecane. n-hexadecane (99.9%) was supplied by Merck (Darmstadt, Germany). In the case of the screening of the pressure, calcination temperature and reaction temperature conditions, the experiments were performed in a stirred tank reactor. In this way temperature and mass transfer resistances were reduced and consumption of reactants was also reduced to a minimum. The temperature was varied in the 200–300 °C range and the total pressure in the 5–25 atm range. The reactor was an all stainless steel vessel, with 0.20 l total volume and a magnetic coupling between the motor and the stirrer. The reaction was carried out in semi continuous mode. The gas flowed continuously while the pressure and flow were maintained in the desired values with the aid of a backpressure regulator and a needle valve. The liquid phase was charged and discharged by removing the flanged reactor head. The gas phase was continuously sampled and analyzed in an on-line Shimadzu GC-8A chromatograph equipped with a flame ionization detector and a 100 m, squalane-coated capillary column. The liquid phase was sample at longer intervals and analyzed off-line in another Shimadzu GC-8A gas chromatograph equipped with a flame ionization detector and a 50 m Phenomenex CP-Sil capillary column. In each experiment 0.5 g of catalyst was first reactivated at 500 °C in air for 1 h to eliminate adsorbed water and then they were reduced in hydrogen at 300 °C for 1 h. The steel reactor was dried in a stove at 110 °C overnight before charging the catalyst. After putting it in the reactor, 26 ml of n-hexadecane were added. The reactor was then closed and tested for leaks under nitrogen pressure. Then it was purged with hydrogen and the pressure was raised to the set point value at room temperature. The reactor was then heated to the reaction temperature and the stirrer was made to spin at 20 Hz. The reaction was performed for the required time and then all connection valves were closed and the reactor was put in a cold water bath to quench the reaction.

The remaining reaction variables (space velocity and H_2/hydrocarbon molar ratio) were studied in a trickle-bed reactor. The hydrogen flow rate was controlled by a high pressure, all-mechanical Cole–Parmer mass flow controller. The total pressure was controlled by a Swagelok backpressure regulator. The liquid flow rate was controlled by an HPLC Cole–Parmer pump. The Reynolds numbers of the liquid and gas phases were adjusted in order to setup a "trickling" flow pattern. To maximize the wetting efficiency the reactor was operated in downflow mode with a bed of catalyst diluted with inert material. The importance of mass transfer resistance and axial dispersion were evaluated with the Weisz–Prater module and the

Peclet number. Both parameters confirmed that neither diffusive limitations nor backmixing was present. A gas–liquid separator after the condenser and backpressure regulator was used to separate the liquid products from the gaseous ones. The latter were periodically sampled in a 6-port valve and finally vented. The liquid phase was sampled and analyzed off-line. Values of n-C_{16} conversion, selectivity and yield to the different products (on a carbon basis) were calculated from chromatographic data. Selectivities were calculated according to the following formula:

$$Si = \frac{Ai.rfi.CNi.100 / MW_i}{X \sum Ai.rfi.CNi / MW_i} \quad (2)$$

where: X is the total conversion, A_i is the chromatographic area of the *ith* compound, rf_i is the response factor of the *ith* compound, CN_i is the carbon number of the *ith* compound and MW_i is the molecular weight of the *ith* compound. The yield is calculated by multiplying the selectivity by the conversion.

2.4. Octane number of the isomerizate

In order to assess the antiknocking properties of the liquid isomerizate the Research Octane Number (RON) was calculated using the composition of the C_{5+} from chromatographic data using a simple non-linear method described elsewhere [27]. The RON gain (ΔRON) of the process was calculated as the difference between the RON of the products mixture and the RON of n-hexadecane.

3. Results and discussion

3.1. Thermodynamics, gasoline quality and molecular features

Gasoline quality most important properties from both environmental and performance points of view are summarized in Table 2. From the required values of volatility of the table it can be seen that no compounds heavier than C_{12}–C_{13} can enter the formulation of gasoline because the end point of the ASTM distillation curve becomes higher than the limit. The maximum value of RVP limits the amount of high volatility short compounds such as branched isopentanes and dissolved butanes. Octane number measures the capacity of a pure compound or a mixture of compounds to resist self ignition by compression at high temperatures.

Octane number depends both on the size and the chemical nature of the compound. Aromaticity, unsaturation, the presence of naphthenic rings and alkyl branching increase the octane number of gasolines. The environmental constraints on the content of benzene and aromatics limit the concentration of these compounds. This leaves isoparaffins as the only component that can be blended to any extent into the reformulated gasoline.

Some values of RON are listed in Table 3. For saturated paraffins the trends of RON with chemical structure are as follows: (i) RON decreases with carbon number; (ii) RON increases with branching. The item (ii) can be further analyzed to deduce that RON increases with the number of quaternary carbon atoms; (iii) RON is increased when branching moves to the center of the molecule (see Fig. 1).

It could seem straightforward to build an "ideal" gasoline by just blending the highest RON compounds while keeping the restrictions on volatility. This is of course not possible due to the unfeasibility of total separation of gasoline compounds but more subtly due to some thermodynamic constraints. If individual compounds are not separated, for cuts of same carbon number a mixture of the isomers is only available. The simplifying hypotheses can be that carbon number cuts are in thermodynamic equilibrium. Hence the average RON of the carbon number cut in thermodynamic equilibrium should be considered (see Fig. 2). The example of the isooctanes is clarifying. Despite the high RON of 2,2,4-trimethylpentane (RON = 100) the average RON of the isooctanes is lower than 50; i.e. high RON compounds are in equilibrium with other low RON ones.

Many conclusions can be drawn from the analysis of the previous figure: (i) C_5–C_7 cuts are the most convenient from a RON point of view. (ii) The mixtures must be obtained at the lowest possible temperature at which thermodynamic equilibrium favors the more branched, higher RON compounds (this is the reason of the negative slope of all curves in Fig. 2).

3.2. Effect of the pretreatment variables on catalyst properties

As the catalysts chosen for the study are commercial ones most variables of the synthesis of the acid support are already fixed. Some remaining variables are the temperature of calcination of the support, the kind of metal function, its amount and conditioning temperature. The most important one is by far the calcination temperature of the support because it highly influences the total amount and distribution of acid sites. These in turn determine the extent of isomerization and cracking. The metal function in oxoanion promoted zirconia has the main purpose of activating hydrogen. Hydrogen participates in reactions of coke hydrogenation, reactions of hydride transfer and surface reactions for the generation of Brönsted dynamic sites. In previous reports of our and other groups many transition metals were tried (Ni, Pt, Pd, etc.) and supported over tungsten–zirconia and sulfated–zirconia supports, for the hydrocracking of medium and long paraffins. All reports conclude that Pt provides the most efficient function [28–31]. Such convenience has generally been put in ambiguous terms. It is generally said that a strong acid function needs of a strong metal function in order to keep an adequate metal/acid balance. In more direct terms Pt produces more active and stable catalysts and for this reason is the metal used in this work. The amount of noble metal and its reduction temperature were chosen in accord with the state of the art for Pt/SZ isomerization catalysts that states that 0.5% Pt and 300 °C are most adequate. This temperature is considered optimum for reducing Pt and preventing the reduction of sulfur.

Catalysts calcined at different temperatures were first characterized by a set of analysis to determine their properties. Chemical analysis was used to determine their composition (Pt, S), nitrogen adsorption to determine their textural properties (specific surface area and pore volume), X-ray diffraction to determine their crystal properties and Py-TPD or Py-FTIR to determine the acid strength and distribution.

Table 2
Premium gasoline specifications (year 2008).

Property	Europe	USA	Japan
Research Octane Number, min.	95	———	96
Sulfur content, max. [ppm]	30	30	10
Benzene content, max. [% Vol.]	5	1	3
Aromatics content, max. [% Vol]	–	25	55
Distillation end point, max. [°C]	225	210	215
Reid vapor pressure, min/max. [psi]	———	2.0–9.0	———

Table 3
RON values of saturated gasoline compounds (of Ref. [49]).

Compound	RON	Compound	RON
n-C_5	62	2-MC_6	42.4
2-MC_4	90	3-MC_6	52
n-C_6	26	3-EC_5	65
2,2-DMC_4	93	2,4-DMC_5	83.1
n-C_8	0	2,3-DMC_5	91.1
2,2,3-TMC_4	112.1	2,2-DMC_5	92.8
n-C_7	0	3,3-DMC_5	80.8

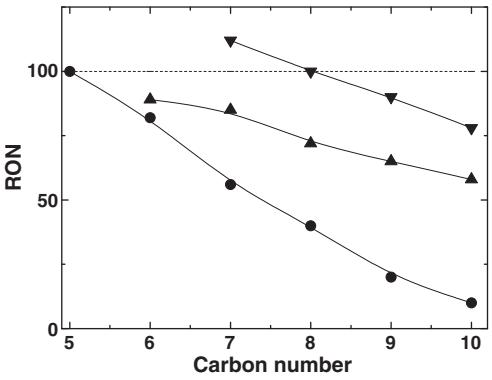

Fig. 1. RON as a function of carbon number for mono (●), di (▲) and tribranched (▼) isomers.

3.2.1. Chemical composition

The chemical analysis results indicated that the percentage of Pt on the three samples studied was 0.5% ± 0.01. This error was considered acceptable. With respect to the sulfur final content (see Table 4) a reduction can be seen at higher calcination temperatures. This reduction of the sulfur content is accompanied by a reduction of the specific area and surface acidity of the catalyst.

3.2.2. Textural and crystal properties

A pore size distribution of the catalyst at different calcination temperatures is included in Fig. 3. The results about the influence of the calcination temperature on the specific surface area (Sg), pore diameter and pore volume (Vp) can be seen in Table 4. It can be seen that an important fraction of the pore structure is microporous (pore size up to 2 nm) while the rest of it is mesoporous (pore size from 2 to 5 nm). No mass diffusion resistances are expected to rise from this pore structure despite the relatively big effective size of the n-hexadecane molecule (5Å). At high calcination temperatures an important decrease of the available surface area and the pore volume can be seen. This is mainly due to the sintering and collapse of micropores that are the main contributors to the total surface area.

The values of BET surface area and sulfur content (Table 4) permit the calculation of the final sulfur surface density of the catalysts as a function of the calcination temperature. It can then be seen that the sulfur surface density is strongly affected by the calcination temperature. Though surface loadings higher than the full monolayer level (4 S nm^{-2}) can be found on uncalcined or mildly heat treated catalysts, for those catalysts calcined at 550–700 °C the reports indicate that sulfur density stabilizes in the half monolayer value (2 S nm^{-2}) and that this value coincides with a maximum of activity of SZ for acid-catalyzed

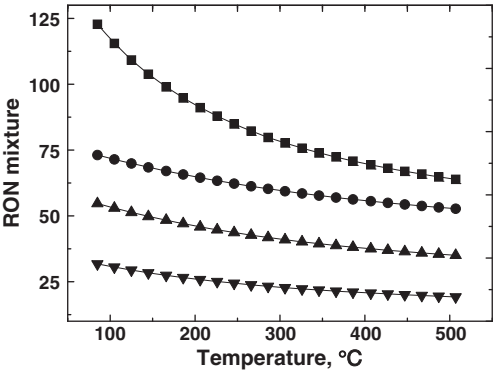

Fig. 2. RON of mixtures of isomers in thermodynamic equilibrium, as a function of the temperature of the mixture. (■) isopentene; (●) isohexane; (▲) isoheptane; (▼) isooctane.

Table 4
Textural and crystal properties of the commercial SO_4^{2-}–ZrO_2 catalyst calcined at different temperatures (SZ^{Tc}).

Catalyst	Composition	Textural properties			Crystal properties	
	S [wt.%]	S_g [m^2g^{-1}]	Dp [nm]	Vp[cm^3g^{-1}]	T [%]	t_C [nm]
XZO	2.8	>300	–	0.3	am.	–
SZ^{600}	2.2	119.0	6.0	0.179	80.1	15.9
SZ^{700}	1.5	103.1	6.2	0.160	69.6	19.8
SZ^{800}	0.8	86.9	6.4	0.139	53.4	15.5

Tc: calcination temperature; Sg: BET specific surface area; Dp: average pore diameter; Vp: pore volume; T: percentage of tetragonality; t_C: crystal size; am.: amorphous.

reactions in the gas phase [32]. For higher temperatures sulfur losses decrease the surface density below the half-monolayer value and lead to destabilization of the crystal structure and loss of catalytic activity [33]. It has been extensively reported in the past that for most sulfated zirconia catalysts calcined at 600–650 °C the stable value of surface sulfur density is approximately half a monolayer [34,35].

XRD spectra of the sulfated zirconia samples calcined at 600, 700 and 800 °C are included in Fig. 4. All spectra show the dominance of the tetragonal habitat over the monoclinic one. However no sample is fully tetragonal. The monoclinic phase, as detected by the peak at 2θ = 28°, has a growing volume fraction in the crystals as the calcination temperature is increased, with a maximum at 800 °C. The dominance of the tetragonal phase, which is not thermodynamically stable in this temperature range, is due to the stabilization of the surface sulfate groups. The mechanism is complex and the controversy still exists. Some authors point to a lattice strain effect induced by the bigger size of sulfo bridges. Other authors indicate that surface sulfate groups are anchored on surface anionic vacancies and stabilize them [36]. These anionic vacancies are formed during the oxolation of the hydroxide gel. Anionic vacancies lower the average coordination number of Zr and contribute to stabilize zirconia into the tetragonal structure which has a coordination number of 8. Otherwise and due to the highly covalent nature of the Zr–O bond the structure is stabilized into the monoclinic habitat with coordination 7 [37]. The transformation of the metastable tetragonal phase into the monoclinic one is known to occur simultaneously with the loss of surface sulfate [38].

3.2.3. Acid properties

Table 5 contains values of amount and strength of acid sites of the catalysts calcined at 600 °C, 700 °C and 800 °C as obtained by pyridine TPD. Föttinger et al. [39], in accord with our results, have observed that the decomposition of sulfate species begin between 625 and 770 °C depending on the sulfur content of the catalyst. They suggest the co-existence of two different types of sulfate groups on the surface. The relative amounts of Brönsted and Lewis sites depend on

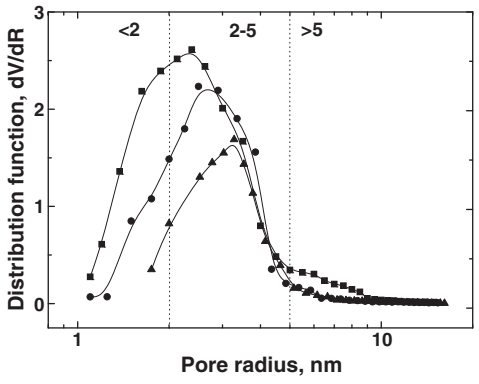

Fig. 3. Pore size distribution of the SO_4^{2-}–ZrO_2 catalyst. (■) Tc = 600 °C; (●) Tc = 700 °C; (▲) Tc = 800 °C.

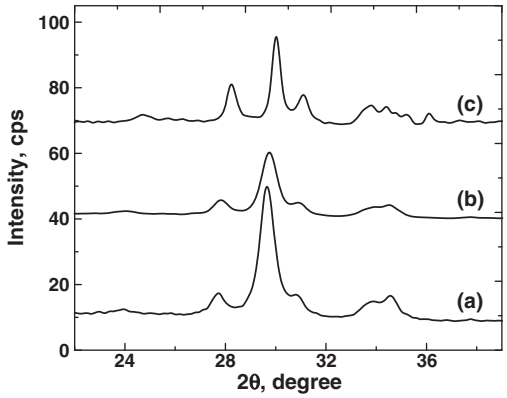

Fig. 4. XRD spectra of the SO_4^{2-}–ZrO_2 catalyst calcined at different temperatures. (a) 600 °C. (b) 700 °C. (c) 800 °C.

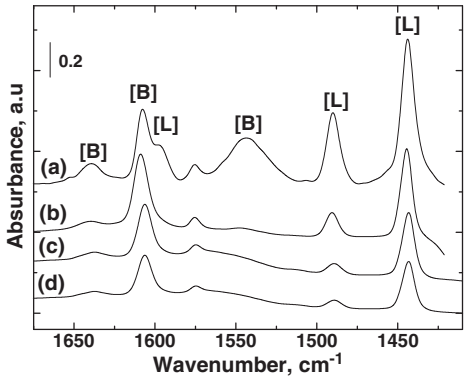

Fig. 5. FT-IR spectra of pyridine adsorbed over commercial SZ catalysts. (a) Calcined at 600 °C and previously reduced in H_2. (b) Calcined at 600 °C, unreduced. (c) Calcined at 800 °C and previously reduced in H_2. (d) Calcined at 800 °C, unreduced. [L]: Lewis acid site. [B]: Bronsted acid site.

the surface concentration of sulfates [40]. Total acidity is decreased as the calcination temperature is increased, in coincidence with a decrease of the mild and strong acid strength and an increase of the amount weak acid sites of the support. This fall coincides with the drop in the sulfur surface density that has been pointed out by many others as the main cause of the acidity decrease [41].

Fig. 5 shows the FTIR spectra of adsorbed pyridine. Pyridine adsorbed over sulfated zirconia has characteristic bands in the 1400–1650 cm^{-1} range. Adsorption on Brönsted sites forms a pyridinium ion with vibration bands at 1638, 1611 and 1540 cm^{-1} while the covalent bond of pyridine on Lewis acid sites yields characteristic bands at 1607, 1486 and 1445 cm^{-1} [42–45]. Table 6 shows results indicating the fraction of Brönsted acid sites (B/(B + L)) and the Brönsted/Lewis (B/L) ratio. The data were obtained by integrating the corresponding intensity bands of Fig. 5. It can be seen that when the calcination temperature is increased both ratios are decreased. This is due both to the dehydration of protonic sites and to the loss of surface sulfate groups and their associated protonic sites. It can also be seen that the treatment in hydrogen on the sample calcined at 600 °C increases the fraction of Brönsted acid sites and the B/L ratio. At higher temperatures the concentration of Lewis acid sites is bigger than the Brönsted one and both ratios decrease. These results are in agreement with those reported by Tran et al. [41] and Föttinger et al. [42].

An overall inspection of the textural, crystalline and acid properties indicates that the sample SZ^{600} seemingly has an optimum of physicochemical properties. However in order to choose appropriate reaction conditions the ultimate test is that of catalytic and selectivity in the reaction test. For this reason the SZ samples were impregnated with Pt and evaluated in the n-hexadecane reaction test. The properties of the metal function were further characterized by cyclohexane dehydrogenation. The metal properties were then correlated with the activity results for the isomerization–cracking of n-hexadecane.

Table 5
Amount and strengh of acid sites on SO_4^{2-}–ZrO_2 catalysts calcined at different temperatures (SZ^{Tc}) as measured by pyridine temperature programmed desorption.

Catalyst	Acidity [mmol Py g^{-1}]			
	Weak	Medium	Strong	Total
	Td < 250	250 < Td < 400	Td > 400	
SZ^{600}	1.0	31.5	106.3	138.8
SZ^{700}	1.7	22.9	91.2	115.8
SZ^{800}	8.6	14.5	25.6	48.7

Tc: calcination temperature; Td: desorption temperature, degrees Celsius.

3.2.4. Metal function properties

The values of catalytic activity and selectivity in the reaction of cyclohexane dehydrogenation are presented in Table 7. It can be seen that Pt over sulfated zirconia has a very small capacity for cyclohexane dehydrogenation, especially if compared with a sample of platinum supported on sulfate-free, tetragonal zirconia calcined at 620 °C (data taken from Ref. [38]). The metal hydrogenating properties increase as the acidity of the support decreases. This is due to the direct relation between the acidity and the metal–support interaction. The sample calcined at 800 °C that had the lowest acidity, was completely selective to the formation of benzene. The loss of metal properties by Pt particles supported over SZ has been extensively reported though the exact mechanism is still a matter of debate [46].

Cyclohexane is a non-demanding reaction in which the rate is strictly proportional to the number of metal exposed sites. It is usually used for characterizing the de/hydrogenating function of supported metal catalysts. When the metal is deposited over a neutral or low acidity support the reaction proceeds with total selectivity to benzene. When the metal is deposited over a very acid support, methylcyclopentane can also be formed, due to the ring-contraction of intermediate cyclohexene over strong acid sites [47]. The higher the contact time of cyclohexane the higher the yield of methylcyclopentane. The contact time of unsaturated intermediates is very much increased on very acid supports.

3.3. Effect of the reaction variables on the catalytic performance

In order to study the effect of the reaction variables the catalyst chosen for the screening tests was the Pt/SZ^{600} one.

3.3.1. Reaction temperature

The results corresponding to the screening of the temperature for the reaction of n-hexadecane can be seen in Fig. 6. The other variables were kept constant. The reaction products were lumped into the

Table 6
Type and amount of acid sites on Pt/SO_4^{2-}–ZrO_2 catalysts calcined at different temperatures (SZ^{Tc}) as measured by FT-IR of adsorbed pyridine. Influence of the use or a prereduction step in hydrogen ($Pt/SZ^{Tc,\ R300}$) or not (Pt/SZ^{Tc}).

Catalyst	Type of acidity	
	B/L	B/(B + L)
Pt/SZ^{600}	0.34	0.25
$Pt/SZ^{600,\ R300}$	0.82	0.45
Pt/SZ^{800}	0.13	0.11
$Pt/SZ^{800,R300}$	0.13	0.12

R300: reduced at 300 °C; B/L: ratio of the intensities of the bands of pyridine adsorbed over Brönsted and Lewis acid sites. B/(B + L): ratio of the intensity of the Brönsted band to the sum of the intensities of the Brönsted and Lewis bands.

Table 7
Yields of methylcyclopentane (Y_{MCP}) and benzene (Y_{Bz}) and total conversion (X) obtained in the test reaction of dehydrogenation of cyclohexane.

	Y_{MCP} (%)	Y_{Bz} (%)	X (%)
Pt/Z^{620}[a]	–[a]	53.8	53.8
Pt/SZ^{600}	9.9	6.6	16.5
Pt/SZ^{700}	10.8	7.0	17.9
Pt/SZ^{800}	–	53.3	53.3

[a] From Ref [38].

following groups: gases, naphtha, kerosene and hexadecane isomers (iC_{16}). Gases were all C_1–C_4 products while the liquid product contained pentanes and heavier compounds. Naphtha is the cut with normal boiling point between 25 and 170 °C (C_5–C_9) and kerosene the cut boiling at 170–225 °C (C_{10}–C_{15}).

The results indicate that increasing the temperature of reaction produces a peak at 225 °C and then an important drop in the yield to hexadecane isomers while the yield to cracked products is significantly augmented. At mild temperatures of up to 250 °C the cracking in middle positions is favored, thus increasing the yield of naphtha. If the temperature is further increased (>250 °C) the cracking begins to generate light gases and the kerosene fraction is increased. The highest yield to hexadecane isomers occurs at 225 °C.

It seems that the best temperature range for producing the cracking of long paraffins over PtSZ with a minimum of production of light gases is 225–250 °C. At this temperature range the highest yield to naphtha is obtained. Temperatures below or above the 225–250 °C range are not attractive. At temperatures lower than 225 °C the acid activity of the catalyst is too low and the system becomes greatly inhibited for the cracking. At temperatures higher than 250 °C there is excessive cracking of long paraffins over the PtSZ catalyst and kerosene products are abundant. A temperature of 225 °C is then the most convenient for the production of naphtha with a high total liquid yield and a low production of light gases.

3.3.2. Total pressure

The tests were performed varying the total pressure and using a reaction temperature of 225 °C. The effect of raising the pressure from a practical point of view is that of increasing the partial pressure of hydrogen because it composes most of the gas phase and only a minor fraction of the gas phase is occupied by the light gases formed by cracking and other hydrocarbons that have a meaningful vapor pressure at 225 °C. From a kinetic point of view raising the hydrogen partial pressure favors the hydrogenation and hydrocracking reactions. Fig. 7 shows that the global reaction rate (proportional to the conversion) has a positive order in hydrogen. This effect is very clear in the 5–15 atm range. At 20 atm a slowdown of the reaction rate occurs and the curve of the yield to hexadecane isomers reaches a plateau. This occurs simultaneously with the decrease of the kerosene fraction and the increase of the naphtha and light gases fractions. Therefore from the point of view of the cracking to naphtha products the best working pressure is in the 15–20 atm range.

It can therefore be assumed that at the reaction conditions chosen the cracking rate is inhibited by the excessive increase of the pressure. An inhibition of the reaction rate by an increase in the hydrogen partial pressure has been explained by Vu et al. [48] by resorting to the classical bifunctional mechanism. High hydrogen pressures would shift the equilibrium of formation of alkenes, intermediates in the Weisz [49] classical bifunctional mechanism. However, and as it can be deduced from the formulae presented by Vu et al. and Weisz, the rate is not expected to increase with pressure at a constant hydrogen-to-hydrocarbon ratio in the feed. In fact it should be constant or decrease. These results can however be explained on the light of the non-classical bifunctional mechanism as presented by Parera and Figoli and Hattori et al. [50–52]. It can be supposed that the higher hydrogen partial pressure favorably affects the rate of hydride transfer. This is a key final elementary step in the non-classical mechanism. Another possibility is that the higher hydrogen pressure increases the concentration of Brönsted dynamic sites, sites of medium acidity and high isomerizing activity. The formation of new Brönsted sites is done at the expense of strong Lewis acid sites responsible for cracking and coking.

The differences between the classical and non-classical bifunctional mechanisms have been explained elsewhere [50]. At high temperatures only the classical mechanism can occur because the formation of olefins is highly feasible and the main function of the metal particles is only to produce and hydrogenate olefins that are easily reacted over the acid sites due to the high temperature. At low temperatures and with very strong acid catalysts the formation of olefins on the metal sites is scarcely possible due to the inhibited properties of Pt. In this case the main function of the metal is to dissociate hydrogen. Molecular hydrogen reduces surface Lewis sites and increases the Brönsted acidity of the support [52].

Iglesia [53] reported that n-heptane isomerization at 200 °C occurred directly by transformation of the alkanes over acid sites with the concurrence of metal sites. Pt allegedly converted molecular hydrogen into atomic hydrogen that diffused over the surface and was finally transferred to a carbenium ion adsorbed on the acid site. Hydride transfer explains the positive effect of hydrogen. Comelli et al. [54] studied the reaction of n-hexane at 200 °C and observed a positive effect of H_2 that was explained in terms of hydrogen inhibiting the deactivation of the catalyst and modifying the half-life time of the adsorbed carbocations. Duchet et al. [55,56] reacted n-hexane over oxoanion promoted zirconia at 150 °C and they also found a positive

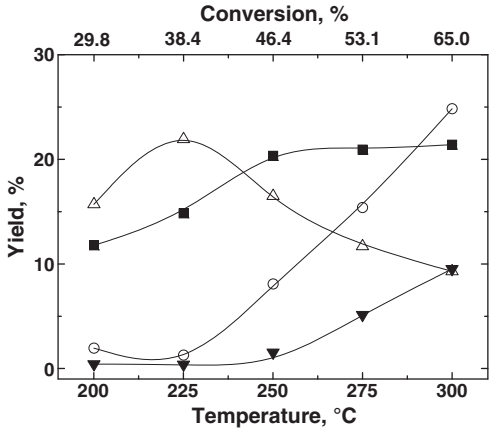

Fig. 6. n-C_{16} reaction on Pt/SZ^{600}, TOS = 180 min, P = 10 atm. Influence of the reaction temperature. (Δ) Hexadecane branched isomers. (■) Naphtha. (○) Kerosene. (▼) Gases.

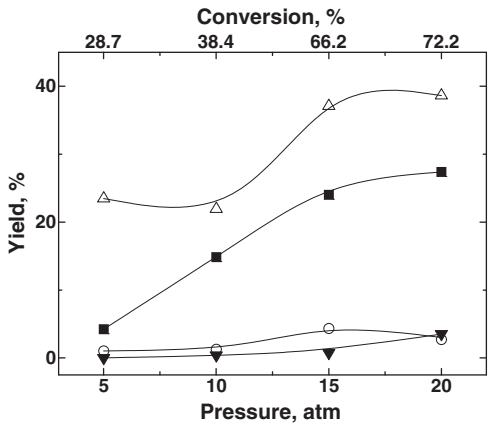

Fig. 7. n-C_{16} reaction on Pt/SZ^{600}, TOS = 180 min, T = 225 °C. Influence of the pressure. (Δ) Hexadecane branched isomers. (■) Naphtha. (○) Kerosene. (▼) Gases.

effect of increasing the hydrogen pressure in the 1–5 bar range. They however supposed that the bifunctional mechanism was not very likely and they instead suggested another mechanism involving Lewis acid sites. Hydride abstraction from n-hexane by the catalyst surface creates carbenium ions that would be adsorbed over Lewis acid sites (oxygen bridge atoms). The adsorbed carbenium ion is highly isomerized and finally desorbed as a paraffin after the hydride transfer occurs. These hydrides are supplied by the homolytic dissociation of hydrogen over Pt particles. The electron transfer on the surface of PtSZ additionally generates (Zr–H−)- and (O–H+) surface species. In this way the higher pressures increase the concentration of surface hydrides and thus accelerate the desorption of carbenium ions and the global reaction rate.

On the same line of reasoning Hattori et al. [51,52,57] suggested that molecular hydrogen is a source of Brönsted acidity. Molecular hydrogen is dissociated over Pt into hydrogen atoms. These migrate by spillover to SZ sites where they are converted into H+ and H−. According to these authors the contribution of the classical bifunctional mechanism during the reactions of paraffins over oxoanion promoted zirconia catalysts would be negligible.

An important detail is the decrease in the rate of formation of hexadecane isomers when the pressure is increased from 15 to 20 atm. A closer look at the results indicates that this decrease occurs in conditions of approximate isoconversion, because from 15 to 20 atm there is only a very small increase in conversion. The global isomerization rate cannot be easily extracted from this figure. However in the reaction mechanism isomerization occurs generally first and cracking afterwards and hence an approximation can be done to obtain the virginal isomerization rate. This is obtained by performing a summation of the yields to all branched isomers. With this approximate estimate we can see that at 15 and 20 atm the yield to all branched isomers is approximately 63%, with a higher contribution of isomers of C_6 and C_7. These results can be interpreted as follows: in the 15–20 atm range the isomerization rate is constant and at 20 atm only the cracking is augmented. The cracking to produce naphtha compounds occurs mainly at the expense of the hexadecane fraction and therefore it can be assumed that cracking occurs in middle positions of the alkyl chain.

The last effect to analyze is that of the slowdown of the pressure effect when going from 15 to 20 atm. A similar and more drastic effect was reported by Busto et al. [58] during the isomerization of n-hexane. According to this report at high partial pressures of hydrogen a phenomenon of competitive adsorption occurs and the effective concentration of surface carbenium ions is decreased because of the blocking of surface sites by hydrogen.

3.3.3. Space velocity

The effect of space velocity on the yield to the different fractions is displayed in Fig. 8. The 4–36 h^{2-1} range was screened. The tests were performed with a constant space velocity throughout the run. The rest of the reaction conditions were: 225 °C, 20 atm and ratio H_2/HC = 6. The figure shows the results corresponding to 60 min TOS. The yields to kerosene and hexadecane isomers were low (<6%). For WHSV = 4 h^{-1} the production of light gases was the highest, 50%. At higher WHSV the yield to gases is decreased and it is reduced to 10% for WHSV = 36 h^{-1}. The yields to the naphtha fraction lie in the 30–40% range. The highest yield is obtained for WHSV = 9 h^{-1}. At higher WHSV values the decrease of the yield is not so important.

Fig. 9 shows the RON gain of the liquid product (ΔRON). This is the difference between the RON values of the C_{5+} mixture and the RON of n-hexadecane. At low contact times there is a decrease of the RON gain due to the main contribution of heavy hydrocarbons of low RON. Fig. 9 contains the values of ΔRON of both the full C_{5+} isomerizate and of the naphtha fraction. It can be seen that for WHSV values lower than 36 h^{-1} higher RON contribution is made by the naphtha fraction. This is in agreement with the introductory discussion about the relation between carbon number and RON (see also Fig. 2). It was concluded there that for the same degree of branching the isomers with higher RON are those with 5–6 carbon atoms. Isomers of higher chain length decrease the relative volatility and increase the heat content. An optimum formulation would be that of an isomerization gasoline with carbon numbers 5–7.

If we compare the results of the last figures, when the space velocity is high (low contact time) the isomerizate has an excessive concentration of long molecules and the degree of branching at any carbon number is low. On the contrary when the contact time is the highest the production of light gases by cracking, especially isobutane, is excessive. In this case the low liquid yield makes this distribution highly undesirable.

3.3.4. Hydrogen-to-hydrocarbon molar ratio

The screening of this variable is mainly motivated by the need of establishing a stable catalyst operation. Therefore the level of conversion must be followed as it varies with the time-on-stream. If the coking rate cannot be counteracted by a similar rate of hydrogenation of coke precursors the conversion is decreased continuously with time-on-stream. If an appropriate hydrogen-to-hydrocarbon ratio is chosen then at some value of time-on-stream the net coking rate becomes null and a pseudo steady-state is reached. This state has an associated constant concentration of coke deposits.

As it can be easily foreseen high hydrogen-to-hydrocarbon ratios favor the stability of the catalyst because decoking rates are increased. However from an economic point of view this ratio should be as small as possible. This is because the hydrocarbon feedstock becomes diluted and the global reaction rate and the throughput are decreased. Hence bigger catalyst loads are necessary for a given conversion or production level. However a most important reason is the costly recycling of high hydrogen volumes. Hydrogen-to-hydrocarbon molar ratios of 1 or lower such as those used in the Penex process allow for a hydrogen once-through configuration, with great savings in the operating cost.

Fig. 10 shows results for different values of the molar ratio H_2/n-C_{16} = 0.5, 6, 10, 15. The other reaction conditions are 225 °C, 20 atm, WHSV = 18.4 h^{-1}. We can see that there is a continuous and drastic deactivation of the catalyst for H_2/n-C_{16} values lower than 10. The minimum, optimal value that assures a complete stability seems to be between 10 and 15. A value of 10 is selected as optimal. This value is much higher than the reported value for the isomerization of short paraffins, which is close to 6. A higher partial pressure of hydrogen is seemingly necessary in this case because of the higher average molecular weight of the feedstock and its tendency to form heavier coke precursors.

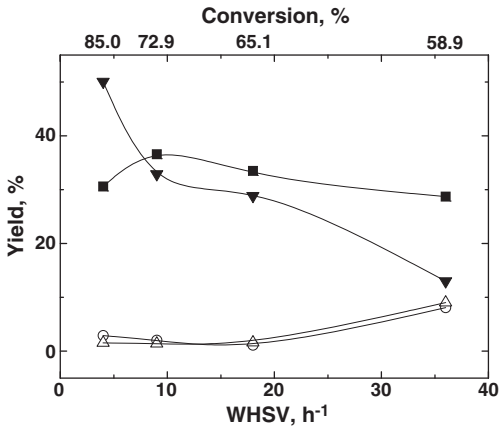

Fig. 8. n-C_{16} reaction on Pt/SZ^{600}, TOS = 60 min, T = 225 °C, P = 20 atm, H_2/HC = 10. Influence of the WHSV. (Δ) Hexadecane branched isomers. (■) Naphtha. (○) Kerosene. (▼) Gases.

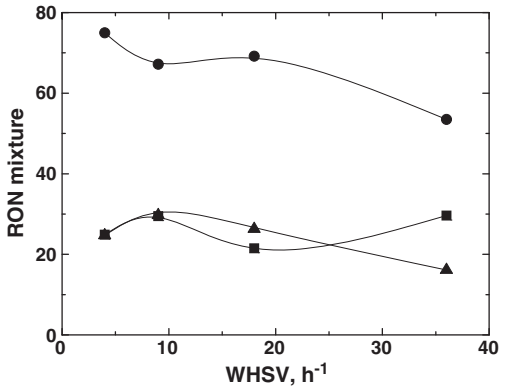

Fig. 9. n-C_{16} reaction on Pt/SZ^{600}, TOS = 60 min, T = 225 °C, P = 20 atm, H_2/HC = 10. RON of the liquid product mixture as a function of the spatial velocity. (●) ΔRON of the whole liquid product; (■) ΔRON of the isomers; (▲) ΔRON of the naphtha fraction.

4. Conclusions

A revision of the theoretical concepts behind the isomerization–cracking of long paraffins indicates that the ideal reaction conditions are those that favor the formation of highly branched isomers in the C_5–C_7 range. Heavier isomerizate compounds like those in the C_8–C_{12} range might have high individual RON values but they are unavoidably accompanied by other compounds of equal carbon number and much lower RON that are part of the thermodynamically equilibrated mixture. Compounds heavier than C_{12} must be reacted or removed due to volatility constraints.

With respect to the assessment of the calcination temperature of PtSZ (screened in the 600–800 °C range) calcination at 600 °C produced the highest activity level while 700 °C was convenient from the point of view of selectivity. The optimum temperature coincided with the production of the highest concentration of Brönsted acid sites.

Regarding the reaction conditions increasing temperature values augmented the conversion but also increased the cracking. Given the high reactivity of the feed, a moderate temperature of 225 °C yielded the best results. Space velocity values were analyzed with attention to the liquid C_{5+} yield, the selectivity to branched isomers and the stability of the catalysts. Best yields to branched naphtha products were obtained at WHSV = 18 h^{-1}. The H_2/hydrocarbon molar ratio was a function of the catalyst coking rate. A value of 10 was enough to attain a stable conversion value. The values of liquid yield as a function of pressure displayed a volcano pattern that was rationalized in terms of a non-classical bifunctional mechanism of reaction. High pressure values increased the concentration of Brönsted acid sites and hence the activity while high pressures enhanced hydrocracking and decreased the liquid yield. The optimal pressure value was 20 atm.

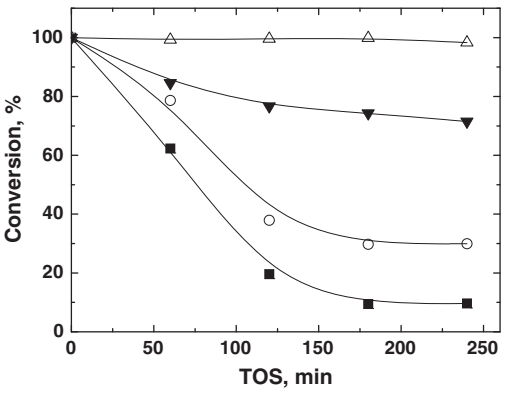

Fig. 10. n-C_{16} reaction on Pt/SZ^{600}, T = 225 °C, P = 20 atm, WHSV = 18.4 h^{-1}. Conversion at a function of time-on-stream (TOS) for different hydrogen-to-hydrocarbon ratios (H_2/n-C_{16}): (■) 0.5; (○) 6; (Δ) 10; (▼) 15.

Acknowledgements

This work was supported with the financial funding of CONICET (PIP 2010–684) and Universidad Nacional del Litoral (CAI + D 2009 II PI 60–296). The authors thank MEL Chemicals for providing sulfated zirconia.

References

[1] V. Calemma, S. Peratello, C. Perego, Hydroisomerization and hydrocracking of long chain n-alkanes on Pt/amorphous SiO_2–Al_2O_3 catalyst, Appl. Catal. A 190 (2000) 207–218.
[2] D. Leckel, Hydrocracking of iron-catalyzed Fischer–Tropsch waxes, Energy Fuels 19 (2005) 1795–1803.
[3] A. Corma, A. Martinez, S. Pergher, S. Peratello, C. Perego, G. Bellusi, Hydrocracking-hydroisomerization of n-decane on amorphous silica-alumina with uniform pore diameter, Appl. Catal. A 152 (1997) 107–125.
[4] K.-C.h. Park, S.-K. Ihm, Comparison of Pt/zeolite catalysts for n-hexadecane hydroisomerization, Appl. Catal. A 203 (2000) 201–209.
[5] W. Zhang, P.G. Smirniotis, Effect of zeolite structure and acidity on the product selectivity and reaction mechanism for n-octane hydroisomerization and hydrocracking, J. Catal. 182 (1999) 400–416.
[6] G. Wang, Q. Liu, W. Su, X. Li, Z. Jiang, X. Fang, C. Han, C. Li, Hydroisomerization activity and selectivity of n-dodecane over modified Pt/ZSM-22 catalysts, Appl. Catal. A 335 (2008) 20–27.
[7] M.C. Claude, J.A. Martens, Monomethyl-branching of long n-alkanes in the range from decane to tetracosane on Pt/H-ZSM-22 bifunctional catalyst, J. Catal. 190 (2000) 39–48.
[8] G. Sastre, A. Chica, A. Corma, On the mechanism of alkane isomerisation (isodewaxing) with unidirectional 10-member ring zeolites. A molecular dynamics and catalytic study, J. Catal. 195 (2000) 227–236.
[9] J. Weitkamp, Isomerization of long-chain n-alkanes on a Pt/CaY zeolite catalyst, Ind. Eng. Chem. Prod. Res. Dev. 21 (1982) 550–558.
[10] J.M. Grau, J.M. Parera, Conversion of heavy n-alkanes into light isomers over H-mordenite, platinum/H-mordenite, platinum/alumina and composite catalysts, Appl. Catal. A 106 (1993) 27–49.
[11] J. Weitkamp, P.A. Jacobs, J.A. Martens, Isomerization and hydrocracking of C_9 through C_{16} n-alkanes on Pt/HZSM-5 zeolite, Appl. Catal. 8 (1983) 123–141.
[12] P. Mériaudeau, V.A. Tuan, V.T. Nghiem, S.Y. Lai, L.N. Hung, C. Naccache, SAPO-11, SAPO-31, and SAPO-41 molecular sieves: synthesis, characterization, and catalytic properties in n-octane hydroisomerization, J. Catal. 169 (1997) 55–66.
[13] J. Walendziewski, B. Pniak, Synthesis, physicochemical properties and hydroisomerization activity of SAPO-11 based catalysts, Appl. Catal. A 250 (2003) 39–47.
[14] S. Lin, H. Ning, S. Wan-Fu, L. Wei-Min, X. Qun-Ji, Preparation of Pd/Al-MCM-41 catalyst and its hydroisomerization properties for long chain alkane compounds, Stud. Surf. Sci. Catal. 141 (2002) 517–524.
[15] S. Zhang, Y. Zhang, J.W. Tierney, I. Wender, Anion-modified zirconia: effect of metal promotion and hydrogen reduction on hydroisomerization of n-hexadecane and Fischer–Tropsch waxes, Fuel Process. Technol. 69 (2001) 59–71.
[16] A. Martínez, G. Prieto, M.A. Arribas, P. Concepción, Hydroconversion of n-hexadecane over Pt/WOx–ZrO_2 catalysts prepared by a PVA-template coprecipitation route. The effect of tungsten surface coverage on activity and selectivity, Appl. Catal. A 309 (2006) 224–236.
[17] Z. Zhou, Y. Zhang, J.W. Tierney, I. Wender, Hybrid zirconia catalysts for conversion of Fischer–Tropsch waxy products to transportation fuels, Fuel Process. Technol. 83 (2003) 67–80.
[18] S. Zhang, Y. Zhang, J.W. Tierney, I. Wender, Hydroisomerization of normal hexadecane with platinum-promoted tungstate-modified zirconia catalysts, Appl. Catal. A 193 (2000) 155–171.
[19] R.A. Keogh, R. Srinivasan, B.H. Davis, The effect of Pt concentration on the activity and selectivity of SO42–ZrO2 catalysts for the hydrocracking and hydroisomerization of n-hexadecane, Appl. Catal. A 140 (1996) 47–57.
[20] M. Busto, V.M. Benítez, C.R. Vera, J.M. Grau, J.C. Yori, Pt-Pd/WO_3–ZrO_2 catalysts for isomerization–cracking of long paraffins, Appl. Catal. A 347 (2008) 117–125.
[21] J.M. Grau, V.M. Benitez, J.C. Yori, C.R. Vera, J.F. Padilha, L.A. Magalhaes Pontes, A.O.S. Silva, Isomerization cracking of n-octane and n-decane on regulated acidity Pt/WOx–SO_4–ZrO_2 catalysts, Energy Fuels 21 (2007) 1390–1395.
[22] H. Deldari, Suitable catalysts for hydroisomerization of long-chain normal paraffins, Appl. Catal. A 293 (2005) 1–10.
[23] J.M. Grau, J.C. Yori, J.M. Parera, Hydroisomerization–cracking of n-octane on Pt/WO_4^{2-}–ZrO_2 and Pt/SO_4^{2-}–ZrO_2. Effect of Pt load on catalyst performance, Appl. Catal. A Gen. 213 (2001) 247–257.
[24] B.-Q. Xu, W.M.H. Sachtler, Reduction of $SO^{=}_4$ ions in sulfated zirconia catalysts, J. Catal. 167 (1997) 224–233.
[25] T. Itoh, Stability of tetragonal phase in ZrO2 powder, J. Mater. Sci. Lett. 5 (1986) 107–108.
[26] E.P. Barrett, L.G. Joyner, P.P. Halenda, The determination of pore volume and area distributions in porous substances. I. Computations from nitrogen isotherms, J. Am. Chem. Soc. 73 (1951) 373–380.

[27] N. Nikolaou, C.E. Papadopoulos, I.A. Gaglias, K.G. Pitarakis, A new non-linear calculation method of isomerisation gasoline research octane number based on gas chromatographic data, Fuel 83 (2004) 517–523.
[28] V.M. Benitez, J.C. Yori, J.M. Grau, C.L. Pieck, C.R. Vera, Hydroisomerization and cracking of n-octane and n-hexadecane over zirconia catalysts, Energy Fuels 20 (2) (2006) 422–426.
[29] C.R. Vera, J.C. Yori, J.M. Parera, Redox properties and catalytic activity of SO_4^{2-}–ZrO_2 catalysts for n-butane isomerization role of transition metal cation promoters, Appl. Catal. A 167 (1998) 75–84.
[30] X. Song, A. Sayari, Sulfated zirconia-based strong solid-acid catalysts: Recent progress, Catal. Rev. Sci. Eng. 38 (3) (1996) 329.
[31] M. Hino, K. Arata, Synthesis of highly active superacids of SO_4/ZrO_2 with Ir, Pt, Rh, Ru, Os, and Pd substances for reaction of butane, Catal. Lett. 30 (1995) 25.
[32] C. Morterra, G. Cerrato, S. Ardizzone, C.L. Bianchi, M. Signoretto, F. Pinna, Surface features and catalytic activity of sulfated zirconia catalysts from hydrothermal precursors, Phys. Chem. Chem. Phys. 4 (2002) 3136–3145.
[33] C.R. Vera, J.C. Yori, C.L. Pieck, S. Irusta, J.M. Parera, Opposite activation conditions of acid and metal functions of Pt/SO_4^{2-}–ZrO_2 catalysts, Appl. Catal. A 240 (2003) 161–176.
[34] C. Morterra, G. Cerrato, C. Emanuel, V. Bolis, On the surface acidity of some sulfate-doped ZrO_2 catalysts, J. Catal. 142 (2) (1993) 349–367.
[35] C.R. Vera, J.M. Parera, Relation between the hydroxylation state of zirconia, the sulfate promotion method, and the catalytic activity of SO_4^{2-}–ZrO_2 catalysts, J. Catal. 165 (1997) 254–262.
[36] R. Srinivasan, Factors influencing the stability of the tetragonal form of zirconia, J. Mater. Res. 1 (4) (1986) 583–588.
[37] C.R. Vera, C.L. Pieck, K. Shimizu, J.M. Parera, Tetragonal structure, anionic vacancies and catalytic activity of SO_4^{2-}–ZrO_2 catalysts for n-butane isomerization, Appl. Catal. A 230 (2002) 137–151.
[38] J.M. Grau, J.C. Yori, C.R. Vera, F.C. Lovey, A.M. Condó, J.M. Parera, Crystal phase dependent metal–support interactions in Pt/SO_4^{2-}–ZrO_2 catalysts for hydroconversion of n-alkanes, Appl. Catal. A 265 (2004) 141–152.
[39] K. Föttinger, K. Zorn, H. Vinek, Influence of the sulfate content on the activity of Pt containing sulfated zirconia, Appl. Catal. A 284 (2005) 69–75.
[40] C. Morterra, G. Cerrato, V. Bolis, Lewis and Brønsted acidity at the surface of sulfate-doped ZrO_2 catalysts, Catal. Today 17 (1993) 505–515.
[41] M.-T. Tran, N.S. Gnep, G. Szabo, M. Guisnet, Influence of the calcination temperature on the acidic and catalytic properties of sulphated zirconia, Appl. Catal. A 171 (1998) 207–217.
[42] K. Föttinger, G. Kinger, H. Vinek, In situ IR investigation of n-hexane isomerization over Pt containing sulfated zirconia, Appl. Catal. A 266 (2004) 195–202.
[43] F. Babou, G. Coudurier, J.C. Vedrine, Acidic properties of sulfated zirconia: an infrared spectroscopic study, J. Catal. 152 (1995) 341–349.
[44] T. Lopez, J. Navarrete, R. Gomez, O. Novaro, F. Figueras, H. Armendariz, Preparation of sol-gel sulfated ZrO_2–SiO_2 and characterization of its surface acidity, Appl. Catal. A 125 (1995) 217–232.
[45] G. Busca, Spectroscopic characterization of the acid properties of metal oxide catalysts, Catal. Today 41 (1998) 191–206.
[46] F. Alvarez, F.R. Ribeiro, G. Perot, C. Thomazeau, M. Guisnet, Hydroisomerization and hydrocracking of alkanes: 7. influence of the balance between acid and hydrogenating functions on the transformation of n-decane on PtHY catalysts, J. Catal. 162 (1996) 179–189.
[47] M.G. Falco, J.M. Grau, N.S. Fígoli, Platinum over tungsten oxide or sulfate promoted zirconia: a study of the metallic and acid functions and their poisoning, Appl. Catal. A 264 (2004) 183–192.
[48] T.N. Vu, J. van Gestel, J.P. Gilson, C. Collet, J.P. Dath, J.C. Duchet, Platinum-tungstated zirconia isomerization catalysts: part II. Effect of platinum and tungsten loading on the mechanism of isomerization of n-hexane: a kinetic study, J. Catal. 231 (2005) 468–479.
[49] P.B. Weisz, in: D.D. Eley, P.W. Selwood, P.B. Weisz (Eds.), Advances in Catalysis and Related Subjects, vol. 13, Academic Press, New York, 1963, p. 157.
[50] J.M. Parera, N.S. Figoli, in: G.J. Antos, A.M. Aitani (Eds.), Catalytic naphtha reforming, 2nd ed., Marcel Dekker, New York, 2004, p. 100.
[51] K. Ebitani, J. Tsuji, H. Hattori, H. Kita, Dynamic modification of surface acid properties with hydrogen molecule for zirconium oxide promoted by platinum and sulfate ions, J. Catal. 135 (1992) 609–617.
[52] T. Shishido, H. Hattori, Spillover of hydrogen over zirconium oxide promoted by sulfate ion and platinum, Appl. Catal. A 146 (1996) 157–164.
[53] E. Iglesia, S.L. Soled, G.M. Kramer, Isomerization of alkanes on sulfated zirconia: promotion by Pt and by adamantyl hydride transfer species, J. Catal. 144 (1993) 238–253.
[54] R.A. Comelli, Z.R. Finelli, S.R. Vaudagna, N.S. Fígoli, Hydroisomerization of n-hexane on Pt/SO42–ZrO2: effect of total and hydrogen partial pressure, Catal. Lett. 45 (1997) 227–231.
[55] J.-C. Duchet, D. Guillaume, A. Monnier, J. van Gestel, G. Szabo, P. Nascimento, S. Decaer, Mechanism for isomerization of n-hexane over sulfated zirconia: role of hydrogen, Chem. Commun. (1999) 1819–1820.
[56] J.C. Duchet, D. Guillaume, A. Monnier, C. Dujardin, J.P. Gilson, J. van Gestel, G. Szabo, P. Nascimento, Isomerization of n-hexane over sulfated zirconia: influence of hydrogen and platinum, J. Catal. 198 (2001) 328–337.
[57] K. Ebitani, J. Konishi, H. Hattori, Skeletal isomerization of hydrocarbons over zirconium oxide promoted by platinum and sulfate ion, J. Catal. 130 (1991) 257–267.
[58] M. Busto, J.M. Grau, S. Canavese, C.R. Vera, Simultaneous hydroconversion of n-hexane and benzene over Pt/WO_3—ZrO_2 in the presence of sulfur impurities, Energy Fuels 23 (2009) 599–606.